Blind Parameter Estimation of M-FSK Signals in the Presence of Alpha-Stable Noise

***Abstract*—Blind estimation of parameters for M-ary frequency-shift-keying (M-FSK) signals is great of importance in intelligent receivers. Many existing algorithms have assumed white Gaussian noise. However, their performance severely degrades when grossly corrupted data, i.e., outliers, exist. This paper solves this issue by developing a novel approach for parameter estimation of M-FSK signals in the presence of alpha-stable noise. Specifically, the proposed method exploits the generalized first- and second-order cyclostationarity of M-FSK signals with alpha-stable noise, which results in closed-form solutions for unknown parameters in both time and frequency domains. As a merit, it is computationally efficient and thus can be used for signal preprocessing, symbol timing estimation, signal and noise power estimation. Furthermore, substantial theoretical analysis on the performance of the proposed approach is provided. Simulations demonstrate that the proposed method is robust to alpha-stable noise and that it outperforms the state-of-the-art algorithms in many challenging scenarios.**

***Index Terms*—alpha-stable noise, generalized cyclostationarity, *M*-ary frequency-shift-keying (*M*-FSK), modulation parameter estimation.**

I. Introduction

BLIND parameter estimation of digital modulation signals is a classical signal processing problem with a wide range of civil and military applications, such as electronic surveillance, signal confirmation, rate allocation, interference identification, monitoring, spectrum management and software defined radio [1]–[3]. In these applications, frequency shift keying (FSK) is widely adopted due to its easy implementation and high immunity to amplitude distortion, especially in short-wave communications and underwater acoustic communications. Accordingly, blind parameter estimation of M-FSK signals has received considerable interest including identification of modulation order, frequency deviation and symbol period.

Over the past two decades, numerous methods have been proposed to tackle blind parameter estimation problem. For example, Ho *et al*. [4] explored the magnitude of wavelet transform to estimate symbol duration for digital signals in Gaussian noise, which was extended later by [5] and [6]. However, the main drawback of these approach is that they require expensive preprocessing such as symbol timing recovery and carrier recovery. Moreover, Liang *et al*. [7] employed the distinct pattern in wavelet transform domain for MFSK signals identification. Then, Chen *et al*. [8] presented a WT-based modulation identifier for MFSK modulation order. Yu *et al* [9] presented a practical algorithm based on the inherent properties of the spectra of MFSK signals for modulation order. El-Mahdy *et al* [10] developed multiple MFSK classifier is based on maximizing the approximated likelihood function. Unlike them, there is a class of methods that employed cyclostationarity in the M-FSK signals for parameter estimation, e.g., [11]–[13] which were based on the first-order cyclostationarity and [14] was based on the second-order cyclostationarity for modulation order and frequency estimation. In addition, the time-frequency analysis is exploited to estimate parameters of FSK signal. In [15], Chee *et al*. presented an estimator based on time-frequency analysis for the instantaneous frequency estimation of FSK signals in AWGN channel. This method exploited the adaptive smooth windowed cross Wigner-Ville distribution to achieve the instantaneous frequency estimation. However, these approaches were developed under Gaussian noise assumption, and thus are not robust to impulsive noise. In other words, when a portion of data is corrupted by heavy-tailed noise such as alpha-stable noise [16]–[19], the above algorithms may suffer severe performance loss. Therefore, it is of great interest to develop robust algorithms for parameter estimation of M-FSK signals.

In the literature, there have been some work achieved satisfactory results in the presence of impulsive noise [20]–[29]. For example, Friedmann *et al*. [20] proposed M-type estimators for the parameters of a deterministic signal, which has the structure of the maximum likelihood estimator. Pelekanakis *et al*. [21] investigated two robust algorithms for sparse channel estimation in the presence of $S\alpha S$ noise. Hu *et al*. [22] proposed a reweighed iterative hard thresholding algorithm for sparse signal recovery in the presence of the $S\alpha S$ Noise.

He *et al*. [23] devised an algorithm for joint estimation of carrier frequency and symbol rate of BPSK signal in the presence of alpha-stable noise. In [24], Yang *et al*. employed explicit myriad cost function and a global optimization method for synchronization parameters estimation of MSK signal in the presence of alpha-stable noise. Nevertheless, the method therein needs the signal and noise power information which unfortunately are difficult to be obtained under alpha-stable noise. Qian *et al*. [25] proposed a block successive upper-bound minimization algorithm for robust frequency estimation by minimizing an l_p-norm cost and proved convergence. However, many of them require hard optimization process and their computational complexities are relatively high. In [26], a new myriad filtering method is proposed to develop communication receiver in the present of $S\alpha S$ noise, which employed an optimal finite impulse response filter to suppress the signal component in the observation data. Hou *et al*. [27] proposed a novel non-data-aided joint estimation algorithm for the time-varying block-memoryless impulsive noise channel. Lu *et al*. [28] proposed a novel system identification algorithm based on the logarithmic least mean p-th power criterion for distributed in-network in alpha-stable noise. Talebi *et al*. [29] considered the characteristic function of $S\alpha S$ signals over sensor networks and derived an optimal filtering solution.

In this paper, we propose a robust estimation algorithm based on the generalized cyclostationarity to estimate the modulation parameters of M-FSK signals in the presence of alpha-stable noise. The main contributions of this paper are summarized as follows.

- We propose new estimators for the modulation order, frequency deviation and symbol period of M-FSK signals by deriving the generalized first- and second-order cyclostationarity of M-FSK signals in symmetric alpha-stable noise.
- We derive the closed-form solutions for parameter estimates in both time and frequency domains, which results in a low-complexity algorithm.
- Our method does not need timing synchronization and signal/noise power estimation.

The remainder of this paper is organized as follows. Section II presents the signal model. Section III introduces a novel algorithm for blind modulation parameter estimation of M-FSK signals. Section IV illustrates the asymptotic properties of the proposed method. Simulation results are given in Section V. Finally, Section VI draws the conclusion.

II. Signal Model

Consider a single input single output system with non-cooperative communication terminals, where after down-conversion, the baseband signal received at time t is given by

$$r(t) = h\left(t\right) \otimes s\left(t\right) + w(t), \tag{1}$$

where $h\left(t\right)$ represents the fading channel, $w(t)$ is the additive noise that is uncorrelated to $s(t)$, and $s(t)$ is the modulated signal which takes the form of

$$s(t) = Ae^{j\theta}e^{j2\pi\Delta f_c t}\sum_i e^{j2\pi f_\Delta s_i t} g\left(t - iT_b\right), \tag{2}$$

where A, θ and Δf_c are the amplitude, phase and frequency offsets, respectively, f_Δ and T_b denote the frequency deviation and symbol period of M-FSK signals, respectively, $g(t)$ is the signal pulse shape, s_i denotes the symbol transmitted within the i-th period, and its value is drawn from a finite alphabet corresponding to the M-FSK modulation, i.e., $s_i \in \left\{\tilde{s}_m \middle| \tilde{s}_m = 2m - 1 - M, m = 1, \cdots, M\right\}$.

We assume that $w(t)$ is alpha-stable distributed with characteristic function defined as follows [30]

$$\varphi\left(u\right) = \exp\left(jeu - \gamma|u|^\alpha\left[1 + j\eta \mathrm{sgn}\left(u\right)\omega\left(u,\alpha\right)\right]\right), \tag{3}$$

where

$$\omega\left(u,\alpha\right) = \begin{cases} -\tan\left(\pi\alpha/2\right), & \alpha \neq 1 \\ \left(2/\pi\right)\log|u|, & \alpha = 1 \end{cases}, \tag{4}$$

$$\mathrm{sgn}\left(u\right) = \begin{cases} 1, & u > 0 \\ 0, & u = 0 \\ -1, & u < 0 \end{cases}. \tag{5}$$

The parameters in (3) are as follows.

- Characteristic exponent α, that controls the heaviness of the tail of the stable density, hence, the smaller the α is, the heavier the tail is.
- Location parameter e, that determines the symmetry center of the probability density function.
- Dispersion parameter γ, that determines the spread of the distribution around the center.
- Index of skewness η, that controls the symmetry of the distribution.

When the stable distribution is symmetric, (3) reduced to

$$\varphi\left(u\right) = \exp\left\{jeu - \gamma|u|^\alpha\right\}. \tag{6}$$

As shown in (6), such symmetric alpha-stable process is denoted as $S\alpha S\left(e,\gamma\right)$. Two well-known alpha distributions are the Cauchy distribution when $\alpha = 1$ and the Gaussian distribution when $\alpha = 2$. It is assumed that $w(t)$ is white noise, a common assumption made for analytical purposes. Additionally, we assume that the samples of the noise process $w(t)$, denoted by $w(t) = w_R(t) + jw_I(t)$, have a bivariate isotropic $S\alpha S$ distribution whose characteristic function is $\varphi\left(u_1,u_2\right) = \exp\left\{-\gamma(u_1^2 + u_1^2)^{\alpha/2}\right\}$. In this paper, the signal and noise power ratio is defined as the mixed signal to noise ratio (MSNR)

$$\mathrm{MSNR} = 10\log_{10}\left(\sigma_s^2/\gamma\right), \tag{7}$$

where σ_s^2 represents the signal variance, and γ represents dispersion coefficient of the alpha-stable noise.

III. Joint Parameter Estimation of M-FSK Signals

The alpha-stable noise has infinite variance when $0<\alpha<2$, and traditional parameter estimators designed for Gaussian noise generally is seriously degraded in this case. The key idea of the algorithm based on generalized cyclostationarity is to construct nonlinear compress function and analyze the generalized cyclostationarity properties of the signal transformed with nonlinear transformation. To begin, let us first derive a useful lemma to illustrate the existence of generalized cyclostationarity.

A. Existence of Generalized Cyclostationarity

Lemma 1: For a symmetric alpha-stable random variable X, the nonlinear compress function is expressed as

$$f[X] = \frac{X}{|X| + \Delta^2}, \tag{8}$$

where Δ^2 represents compression factor and its value tends to zero, but it is not equal to zero.

The n-th moment of $f[X]$ obeys

$$|E\{f^n[X]\}| = \left| E\left\{ \left(\frac{X}{|X| + \Delta^2} \right)^n \right\} \right| \leq 1, \tag{9}$$

where $E\{\cdot\}$ is the expectation operator.

Proof: See Appendix A. ∎

Remark 1: For a alpha-stable random variable X, the nonlinear compress function makes the generalized high order moment of X exist, that is $f[X]$ has high order moment in Lemma 1.

B. Properties of Generalized Cyclostationarity

Now let us focus on the derivations of some useful properties of generalized cyclostationarity, which will be used to derive our method. Our results are drawn as follows:

Proposition 1: The received FSK signal exhibits generalized first-order cyclostationarity and the number and position of the first-order cycle frequencies are dependent on the modulation order M and frequency deviation f_Δ.

Proof: See Appendix B. ∎

Proposition 2: The received FSK signal exhibits generalized second-order cyclostationarity and the peak pattern of generalized second-order cyclic moment magnitude is dependent on the symbol period T_b.

Proof: See Appendix C. ∎

C. Proposed Estimation Algorithm

The generalized first-order time-varying moment of $r(t)$ is defined as

$$C_r(t) = E\{f[r(t)]\}, \tag{10}$$

where $f[r(t)] = \frac{r(t)}{|r(t)|+\Delta^2}$. If $C_r(t)$ is approximately a periodic function of time, the signal $r(t)$ is generalized first-order cyclostationary process and $C_r(t)$ has a Fourier series expansion as

$$C_r(t) = \sum_{\tilde{\varepsilon} \in \kappa} \tilde{\vartheta}_r(\tilde{\varepsilon}) e^{j2\pi\tilde{\varepsilon}t}, \tag{11}$$

where κ represents the set of first-order cycle frequencies (CFs). $\tilde{\vartheta}_r(\tilde{\varepsilon})$ is the generalized first-order cyclic moment (CM) at cycle frequencies $\tilde{\varepsilon}$, which is defined as

$$\tilde{\vartheta}_r(\tilde{\varepsilon}) = \lim_{T\to\infty} T^{-1} \int_{-T/2}^{T/2} C_r(t) e^{-j2\pi\tilde{\varepsilon}t} dt. \tag{12}$$

For the discrete-time signal $r(k) = r(t)|_{t=kf_s^{-1}}$, by sampling the continuous-time signal $r(t)$ at a sampling rate f_s, the generalized first-order cyclic moment and corresponding set of cycle frequencies become

$$\vartheta_r(\varepsilon) = \tilde{\vartheta}_r(\varepsilon f_s), \tag{13}$$

$$\kappa = \left\{ \varepsilon : \varepsilon \in [-0.5, 0.5), \varepsilon = \tilde{\varepsilon} f_s^{-1}, \vartheta_r(\varepsilon) \neq 0 \right\}. \tag{14}$$

The generalized second-order time-varying moment of the received signal $r(t)$ is expressed as

$$G_r(t, \tilde{\tau}) = E\{f[r(t)] f^*[r(t - \tilde{\tau})]\}, \tag{15}$$

where $\tilde{\tau}$ denotes the time delay, and * represents the complex conjugate. If $G_r(t, \tilde{\tau})$ is an (almost) periodic function of time, the signal $r(t)$ exhibits generalized second-order cyclostationarity, and $G_r(t, \tilde{\tau})$ is decomposed by a Fourier series as

$$G_r(t, \tilde{\tau}) = \sum_{\tilde{\beta} \in \psi} \tilde{\Omega}_r(\tilde{\beta}, \tilde{\tau}) e^{j2\pi\tilde{\beta}t}, \tag{16}$$

where ψ is the set of the second-order cycle frequencies (CFs). $\tilde{\Omega}_r(\tilde{\beta}, \tilde{\tau})$ is the generalized second-order cyclic moment (CM) at cycle frequencies $\tilde{\beta}$, and is expressed as

$$\tilde{\Omega}_r(\tilde{\beta}, \tilde{\tau}) = \lim_{T\to\infty} T^{-1} \int_{-T/2}^{T/2} G_r(t, \tilde{\tau}) e^{-j2\pi\tilde{\beta}t} dt. \tag{17}$$

For the discrete-time signal $r(k) = r(t)|_{t=kf_s^{-1}}$, the generalized second-order cyclic moment and corresponding set of cycle frequencies are given by

$$\Omega_r(\beta, \tau) = \tilde{\Omega}_r\left(\beta f_s, \tau f_s^{-1}\right), \tag{18}$$

$$\psi = \left\{ \beta : \beta \in [-0.5, 0.5), \beta = \tilde{\beta} f_s^{-1}, \Omega_r(\beta, \upsilon) \neq 0 \right\}. \tag{19}$$

According to Proposition 1, $\tilde{\vartheta}(\tilde{\varepsilon})$ exhibits peaks for $\tilde{\varepsilon} \in \{\tilde{\varepsilon} = \Delta f_c + \rho T_b^{-1}, \rho = \pm l, \cdots, \pm(M-1)l, l \in Z\}$ if $f_\Delta = lT_b^{-1}$, and the number of the first-order cycle frequencies $\tilde{\varepsilon}$ equals the modulation order M. In addition, the distance between adjacent first-order cycle frequencies $\tilde{\varepsilon}$ is dependent on the tone frequency spacing f_Δ, that is $|\tilde{\varepsilon}_i - \tilde{\varepsilon}_{i+1}| = 2f_\Delta$. Based on Proposition 2, the absolute value of $\tilde{\Omega}(0, \tau)$ exhibits periodic peaks at $\tilde{\beta} \in \left\{ \tilde{\beta} = lT_b^{-1}, l \in Z \right\}$. The value of $\left| \tilde{\Omega}(0, \tilde{\tau}) \right|$ decreases when the delay increases for $\tilde{\tau} < T_b$, and it remains constant when $\tilde{\tau} \geq T_b$. In other words, the second-order cyclic moment magnitude exhibits the property that a change in the peak pattern at a delay is equal to the symbol period. Based on the above analysis, a blind algorithm for modulation parameter estimation of M-FSK signals can be developed for alpha-stable noise. The proposed algorithm consists of the following steps.

Step 1. The received signal $r(t)$ is sampled at a sampling rate f_s, that is $r(k) = r(t)\Big|_{t=kf_s^{-1}}$. The sampling rate f_s is set large enough in the case of no priori information about the signal bandwidth B, that is $f_s \geq \varsigma B$ ($\varsigma \geq 2$). The sampled signal is defined as

$$r(k) = h(k) \otimes s(k) + w(k), \tag{20}$$

where $h(k)$ represents the fading channel, $s(k) = s(t)\Big|_{t=kf_s^{-1}}$ and $w(k) = w(t)\Big|_{t=kf_s^{-1}}$ represent the complex modulated signal and complex alpha-stable noise, respectively.

Step 2. $r(k)$ is transformed as $f[r(k)] = \frac{r(k)}{|r(k)|+\Delta^2}$, and the estimator of generalized first-order cyclic moment $\hat{\vartheta}_r(\varepsilon)$

at cycle frequencies, is given as

$$\hat{\vartheta}_r(\varepsilon) = \frac{1}{K}\sum_{k=0}^{K-1} f[r(k)]\, e^{-j2\pi\varepsilon k/K}. \quad (21)$$

Step 3. The cycle frequencies are selected to obtain a set of candidate frequencies. We first calculate a statistic $\Gamma_\vartheta = \frac{\max[Q]}{\bar{\vartheta}+\varpi}$ for all frequencies, where $\bar{\vartheta} = E\left\{\hat{\vartheta}_r(\varepsilon)\right\}$, $\varpi = \sqrt{E\{\left[\hat{\vartheta}_r(\varepsilon) - \bar{\vartheta}\right]^2\}}$, and Q represents a set and its initial value is $Q = \left\{\hat{\vartheta}_r(\varepsilon)\right\}$. Then, we set a cutoff value δ, and compare δ to Γ_ϑ. If the cutoff value δ is below the statistic Γ_ϑ, the frequency ε that maximizes the statistics Γ_ϑ is believed to be a candidate frequency. Besides, the set Q is updated by removing the candidate frequency selected in the previous step. Because of the cycle frequency resolution, the discrete spectral lines are usually not a set of multiple lines at cycle frequency. In order to suppress the effect of irregular chaotic lines at the next cycle frequency, the spectral line value within the set $[\varepsilon-\nu, \varepsilon+\nu]$ (where $\nu > 0$) is set zero. Finally, by repeating the above process, we obtain a set of cycle frequencies $\hat{\kappa}$.

Step 4. The modulation order M and tone frequency spacing f_Δ are estimated. The number of the first-order cycle frequencies decisions the M-FSK modulation order. For example, the received signal is estimated as 2-FSK, when the number of first-order cycle frequencies is two. The received signal is considered to be M-FSK ($M = 2^m, M \geq 4$) if at least $2^{m-1}+1$ first-order cycle frequencies are detected. The decision on the M-FSK tone frequency spacing is based on the minimum distance between adjacent cycle frequencies, that is $\hat{f}_\Delta = \Delta\varepsilon f_s/2$, where $\Delta\varepsilon = \arg\min_{\kappa} |\varepsilon_i - \varepsilon_j|$.

Step 5. The estimate of generalized second-order cyclic moment at cycle frequencies β, is calculated

$$\hat{\Omega}_r(\beta,\tau) = \frac{1}{K}\sum_{k=0}^{K-1} f[r(k)]\, f^*[r(k+\tau)]\, e^{-j2\pi k\beta/K}. \quad (22)$$

Step 6. The symbol period is estimated. According to the Proposition 2, the magnitude of $\left|\tilde{\Omega}\left(0, l\left(2f_\Delta\right)^{-1}\right)\right|$ remains constant when $\left|l\left(2f_\Delta\right)^{-1}\right| \geq T_b$. Substituting the minimum distance between adjacent cycle frequencies into $\hat{\Omega}_r(\beta,\tau)$ gives $\left|\hat{\Omega}_r\left(0, l\left(\Delta\varepsilon\right)^{-1}\right)\right|$. Let $S_\iota = \left|\Omega\left(0, \iota\left(\Delta\varepsilon\right)^{-1}\right)\right|$ $\left(\iota = 0, 1, \cdots, v_{\max}\right)$, and let F be a variable with initial value $S_{v_{\max}}$. We define the variable sets H and D, and initialize them by using $\left\{V_{v_{\max}}\right\}$ and $\left\{V_1, V_2, \cdots, V_{v_{\max}-1}\right\}$, respectively. For $v = 1$ to $v_{\max}$, V_v is calculated sequentially, that is $V_v = \arg\min_{V_\iota \in D}\left|V_\iota - F\right|$. If $\left|V_v - F\right| < \sigma$, then $D = D \cap \overline{\left\{V_v\right\}}$, $H = \left\{V_{v_{\max}}\right\} \cup H$ and $F = E\{H\}$, otherwise break. The set H member of minimum delay provides the estimate of the symbol period T_b, that is $\hat{T}_b = \frac{\hat{\tau}}{f_s}$ ($\hat{\tau} = \arg\min_{\iota\cdot\left(\Delta\varepsilon\right)^{-1}} \left\{H\right\}$) [14].

The procedure of blind parameter estimation for M-FSK signals with alpha-stable noise is summarized in Algorithm 1.

Algorithm 1 Blind parameter estimation for M-FSK signals with alpha-stable noise.

1: Initialize parameters Δ, δ, ν and σ.
2: Sample received signal at a rate of f_s, that is $r(k) = r(t)\Big|_{t=kf_s^{-1}}$.
3: Map $r(k)$ by the nonlinear function, that is $f[r(k)] = \frac{r(k)}{|r(k)|+\Delta^2}$.
4: Calculate generalized first-order cyclic moment $\hat{\vartheta}_r(\varepsilon)$ using (21).
5: Select the first-order cyclic frequencies κ.
6: Identify the modulation order M, and tone frequency spacing f_Δ by first-order cyclic frequencies set κ.
7: Calculate generalized second-order cyclic moment $\hat{\Omega}_r(\beta,\tau)$ using (22).
8: Estimate the symbol period by employing $\hat{\tau} = \arg\min_{i\cdot(\Delta v)^{-1}}\{H\}$ and $\hat{T}_b = \frac{\hat{\tau}}{f_s}$.

D. Asymptotic Properties of the Proposed Algorithm

We note that in our method, the tone frequency spacing is estimated by detecting the first-order cycle frequencies, while the symbol period is determined by extracting the second-order cycle frequencies. They are related to the first- and second-order generalized cyclic moments, respectively. It is important to check if our method is statistically meaningful. The following two propositions show that the parameter estimates of our algorithm are asymptotically unbiased and consistent.

Proposition 3: The estimator of $\hat{\vartheta}_s(\varepsilon)$ is asymptotic unbiased and consistent.

Proof: See Appendix D. ■

Proposition 4: The estimator of $\hat{\Omega}_s(\beta, \upsilon)$ is asymptotic unbiased and consistent.

Proof: See Appendix E. ■

IV. Simulation Results

In this section, the performance of the proposed generalized cyclostationarity-based algorithms is evaluated in the presence of alpha-stable noise. We consider M-FSK signals, with modulation order $M = 2, 4, 8$, a symbol rate of $f_b = T_b^{-1}$ and a single-sided bandwidth of 2 KHz. The sampling rate f_s is 25 KHz, and the frequency offset Δf_c equals 1000 Hz. Unless otherwise stated, the observation period is 0.5 sec, which corresponds to 500 2FSK symbols, 250 4FSK symbols, or 125 8FSK symbols, respectively. All results are calculated based on 1000 Monte Carlo trials. The probability of correct estimation P_{ce} is employed to examine the estimation performance of our method. Specifically, for modulation order estimation, we follow [11] to calculate P_{ce} via

$$\Pr\left[M = \hat{M}\right], \quad (23)$$

where $\hat{M}$ is the estimate of M. For tone frequency spacing and symbol period, we follow [31] and [14], and calculate P_{ce} as

$$\Pr\left[|Y - \hat{Y}|/Y \leq 10^{-2}\right], \quad (24)$$

where $\hat{Y}$ is the estimate of Y.

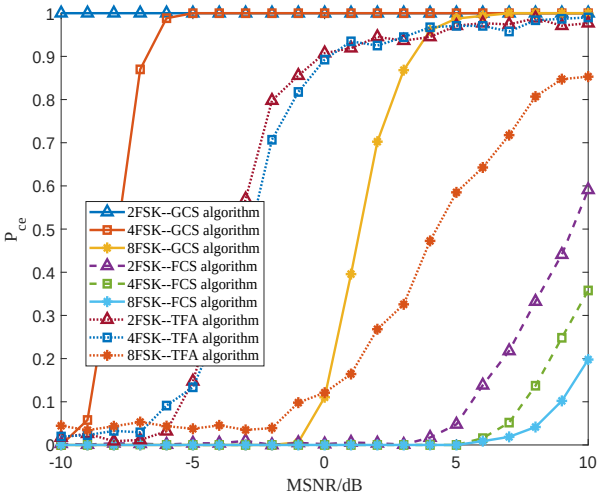

Fig. 1. Modulation order estimation performance versus different MSNRs

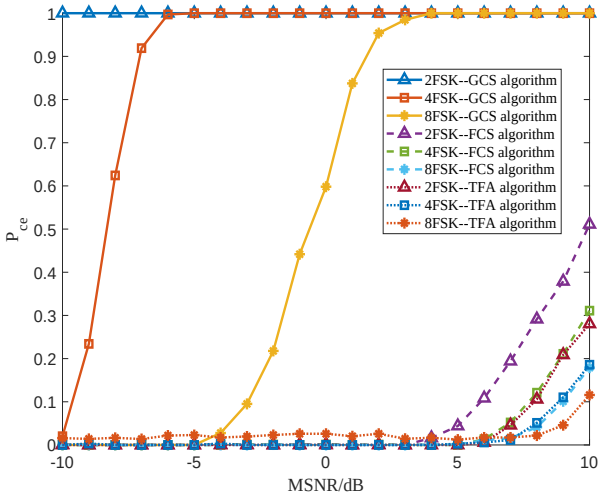

Fig. 2. Tone frequency spacing estimation performance versus different MSNRs

A. Performance of Proposed Estimation Algorithm

We examine how P_{ce} of our method varies by changing MSNR. We choose the modulation order $M \in (2, 4, 8)$. We compare our generalized cyclostationarity-based algorithm (GCS) with first-order cyclostationarity-based algorithm (FCS) in [11] and the time-frequency analysis-based algorithm (TFA) in [15]. The results are plotted in Figs. 1 and 2, where the former is for modulation order estimation while the latter is for frequency deviation estimation. One sees that TFA and FCS do not perform well in alpha-stable noise since they are unable to deal with heavy-tailed noise. But GCS performs well in both cases. For example, in Fig 1, its P_{ce} reaches 1 for 2FSK signals, even in low SNR cases. For 8FSK signals, when MSNR is greater than 4 dB, GCS offers $P_{ce} = 1$ while the other methods failed to work. Note that the complexity of the GCS algorithm is $O(NlogN)$ while that of the FCS and TFA algorithms are in the same order as GCS. So our method is more appealing since it achieves the higher performance but with almost the same complexity as FCS and TFA.

In Fig. 3, the probability of correct symbol period estimation, for $M = 2, 4, 8$, is plotted versus MSNR. For reference, the performance of the second-order cyclostationarity-based algorithm (SCS) in [14] and the wavelet transform-based algorithm (WT) in [6] with symmetric alpha-stable noise are also plotted in these figures. From Fig. 3, it can be shown that the proposed algorithm is robust against symmetric alpha-stable noise and significantly outperforms the existing algorithms. Moreover, for given higher MSNR, the performance of 8FSK signal is worse than that of 4FSK and 2FSK. This is because that in such cases, the performance of symbol period is affected by the tone frequency spacing estimation. In addition, the complexity of the proposed GCS algorithm is compared with the SCS and WT algorithms. For the number of samples N, the calculation complexity for GCS algorithm is $O(NlogN)$ and the SCS and TFA algorithm also have order $O(NlogN)$. It showed that the proposed GCS yields significant performance gains under the same computational complexity.

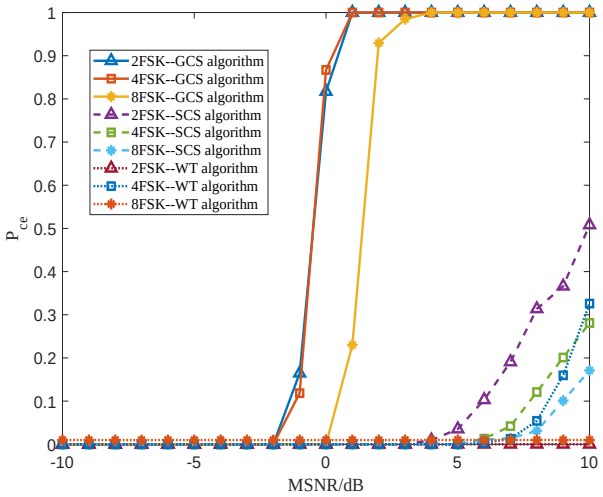

Fig. 3. Symbol period estimation performance versus different MSNRs

Fig. 4 shows the probability of correct symbol period estimation. We see that the proposed algorithm performs well under different settings, especially for 2FSK signal and 4FSK signal, where its performance with estimated f_Δ is close to that with true f_Δ. However, compared to 2FSK and 4FSK signals, estimating f_Δ for 8FSK signals is more difficult, so our method showed relatively poor performance.

In addition, the CRB and mean square error of the proposed and the existing algorithms are compared in Figs. 5-6. In Fig. 5, the mean square error of the tone frequency spacing estimation are plotted versus MSNR for 4FSK. From Fig. 5, it can be shown that the proposed algorithm is robust against symmetric alpha-stable noise and significantly outperforms the existing algorithms when MSNR is greater than -4dB. In Fig. 6, the mean square error of the symbol period estimation for 4FSK is plotted versus MSNR. From Fig. 6, it is observed that the existing algorithms behave poorly in presence of

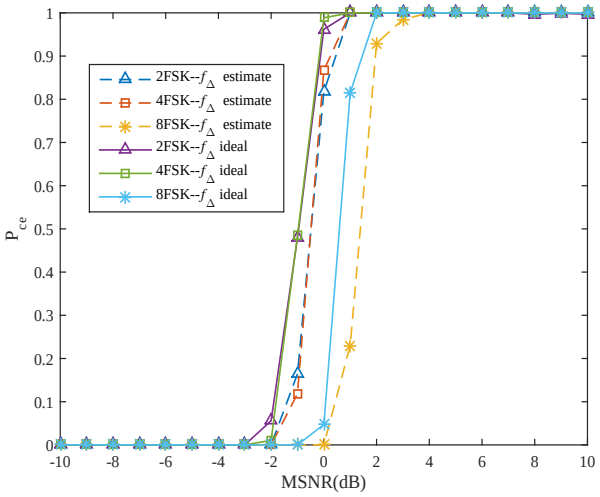

Fig. 4. Symbol period estimation performance with different f_Δ versus different MSNRs

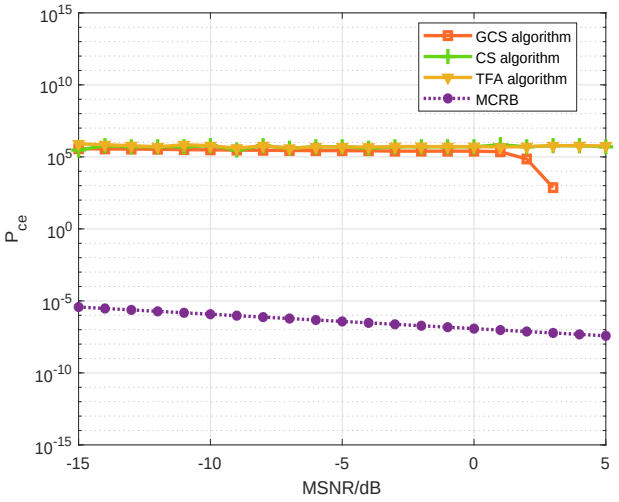

Fig. 6. The mean square error of the symbol period estimation.

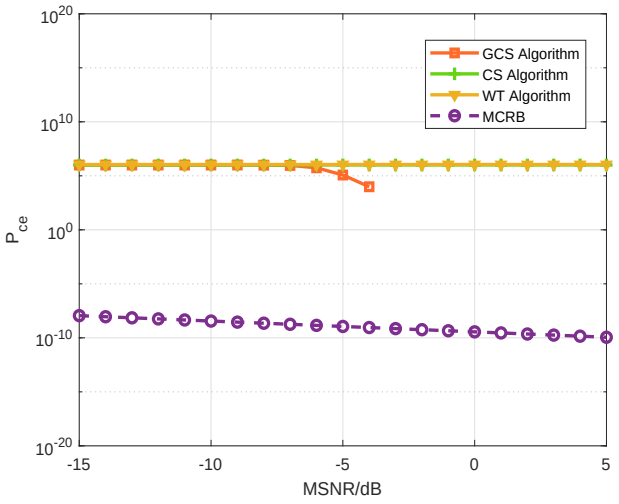

Fig. 5. The mean square error of the tone frequency spacing estimation.

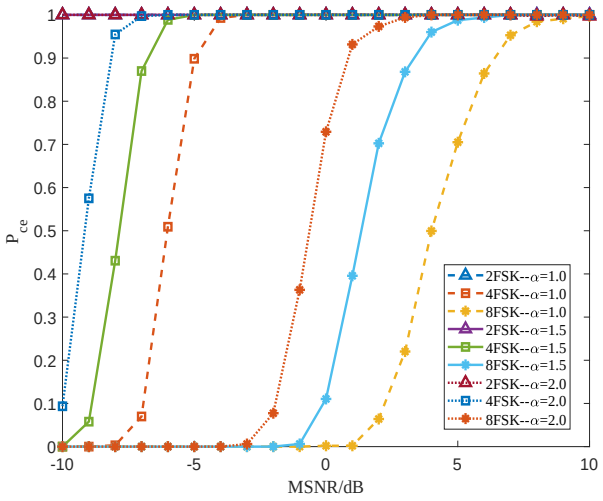

Fig. 7. The P_{ce} of the modulation order versus MSNR, with different α values

symmetric alpha-stable noise, but the proposed algorithm is reasonably robust against symmetric alpha-stable noise under higher MSNR conditions.

B. Effect of Noise Parameters on Algorithm Performance

In this example, we study how the parameter alpha affects the performance of the proposed algorithm. Specifically, the effects of the parameter α on the value of P_{ce} for modulation order, tone frequency spacing and symbol period will be shown in Figs. 7-9, respectively. It can be seen that a larger α results in higher probability for the proposed method. Moreover, it is worth mentioning that our method performs well in many challenging scenarios such as $\alpha = 1$ with which the noise distribution is pretty heavy-tailed and more outliers can be generated to corrupt the signal. When $\alpha = 2$, our method also shows reasonably well performance.

V. Conclusion

We have proposed a new method for blind parameter estimation of M-FSK signals in alpha-stable noise. Our method is based on the so-called generalized cyclostationary properties proved in this paper. We have derived closed-form expressions for the parameter estimation including modulation order, frequency deviation and symbol period. Theoretical analysis and numerical experiments have shown the effectiveness and robustness of the proposed method over the state-of-the-art algorithms.

Appendix A
Proof of Lemma 1

According to (8), we can obtain

$$|f[X]| = \left|\frac{X}{|X| + \Delta^2}\right| \leq \left|\frac{X}{|X|}\right| = 1. \tag{25}$$

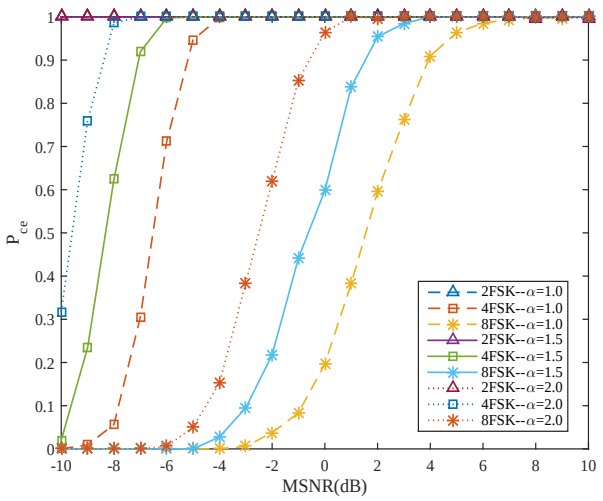

Fig. 8. The P_{ce} of the tone frequency spacing versus MSNR, with different α values

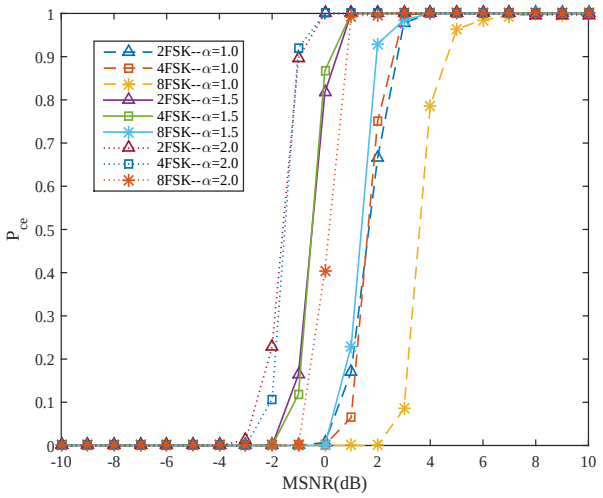

Fig. 9. The P_{ce} of symbol period versus MSNR, with different α values

Furthermore

$$|f[X]|^n = \left|\frac{X}{|X|+\Delta^2}\right|^n \le \left|\frac{X}{|X|}\right|^n = 1. \tag{26}$$

The n-th moment of $|f[X]|$ is given by

$$E\{|f[X]|^n\} = E\left\{\left|\frac{X}{|X|+\Delta^2}\right|^n\right\} \le E\left\{\left|\frac{X}{|X|}\right|^n\right\} = 1. \tag{27}$$

For $n \ge 1$, we get the following conclusion

$$\begin{aligned} E\left\{\left(\frac{X}{|X|+\Delta^2}\right)^n\right\} &\le E\left\{\left|\left(\frac{X}{|X|+\Delta^2}\right)^n\right|\right\} \\ &\le E\left\{\left|\frac{X}{|X|+\Delta^2}\right|^n\right\} \le 1. \end{aligned} \tag{28}$$

Appendix B
Proof of Proposition 1

To simplify the proof of Proposition 1, we first present a useful Lemma.

Lemma 2: If the product $f_\Delta \tilde{s}_m$ is an integer of T_b^{-1}, the generalized first order cyclic moment of the received M-FSK signals can be expressed as

$$\tilde{\vartheta}(\tilde{\varepsilon}) = \Im\{C_r(t)\} \approx \Lambda_i \sum_{\rho\in \mathrm{P}} \delta\left(\tilde{\varepsilon} - \Delta f_c - \rho T_b^{-1}\right), \tag{29}$$

where $\Im\{\cdot\}$ denotes the Fourier transform, $\Lambda_i \in [\Lambda_h, \Lambda_l]$, $\Lambda_h = \frac{\rho_h A e^{j\theta} M^{-1}}{|\rho_h A|+\Delta^2}$, $\Lambda_l = \frac{\rho_h A e^{j\theta} M^{-1}}{|w(t)|+\Delta^2}$ and $\{\rho = f_\Delta \tilde{s}_m T_b, \rho \in Z, \tilde{s}_m = 2m-1-M\}$.

Proof: See Appendix F. ∎

Based on Lemma 2, we assume that $f_\Delta = lT_b^{-1}$, with l as an integer, the equation (29) can be rewritten as

$$\tilde{\vartheta}(\tilde{\varepsilon}) = \Im\{C_r(t)\} \approx \sum_{\rho\in\{\pm l,\cdots,\pm(M-1)l\}} \Lambda_i \delta\left(\tilde{\varepsilon} - \Delta f_c - \rho T_b^{-1}\right). \tag{30}$$

where $\{\rho = l\tilde{s}_m = \pm l, \cdots, \pm(M-1)l, l \in Z\}$.

According to (30), it is noteworthy that $\tilde{\vartheta}(\tilde{\varepsilon}) \ne 0$ with $\tilde{\varepsilon} \in \left\{\tilde{\varepsilon} = \Delta f_c + \rho T_b^{-1}, \rho = \pm l, \cdots, \pm(M-1)l, l \in Z\right\}$ and the magnitude of $\tilde{\vartheta}(\tilde{\varepsilon})$ decreases with an increase in modulation order M. In addition, the number of first-order cycle frequencies is equal to the modulation order M, and the cycle frequencies is dependent on the frequency offset Δf_c and frequency deviation f_Δ.

Appendix C
Proof of Proposition 2

To simplify the proof of Proposition 2, Lemma 3 is presented as follows.

Lemma 3: The analytical expressions of the generalized second-order cyclic moment of the M-FSK signals can be given as

$$\tilde{\Omega}_r\left(\tilde{\beta},\tilde{\tau}\right) = \begin{cases} \Re_i (T_b M)^{-1} e^{j2\pi\Delta f_c \tilde{\tau}} \sum_{p=1}^{M} e^{j2\pi f_\Delta \tilde{s}_p \tau_0} \Big(U_1\left(\tilde{\beta}\right) \\ +M^{-1}\sum_{q=1}^{M} U_2\left(\tilde{\beta} - (\tilde{s}_q - \tilde{s}_p) f_\Delta\right)\Big), \\ \quad \text{when} \quad |\tilde{\tau}| < T_b \\ \Re_i T_b^{-1} M^{-2} e^{j2\pi\Delta f_c\tilde{\tau}} \\ \sum_{q=1}^{M}\sum_{p=1}^{M} e^{j2\pi f_\Delta \tilde{s}_p \tau_0}\Big(U_1\left(\tilde{\beta} - (\tilde{s}_q - \tilde{s}_p) f_\Delta\right) \\ +U_2\left(\tilde{\beta} - (\tilde{s}_q - \tilde{s}_p) f_\Delta\right)\Big), \\ \quad \text{when} \quad |\tilde{\tau}| \ge T_b \end{cases}, \tag{31}$$

where $\Re_i \in [\Re_h, \Re_l]$, $\Re_h = \frac{(\rho_h A)^2}{|\rho_h A|^2+\Delta^2}$, $\Re_l = \frac{(\rho_h A)^2}{|w(t)|^2+\Delta^2}$, $U_1\left(\tilde{\beta}\right)$ and $U_2\left(\tilde{\beta}\right)$ are the Fourier transforms of $g(t)g(t-\tau_0)$ and $g(t)g(t+\mu T_b-\tau_0)$.

Proof: Appendix G. ∎

Based on Lemma 3, we notice that $\tilde{\Omega}_r\left(\tilde{\beta},\tilde{\tau}\right)$ exhibits peaks for $\left\{\tilde{\beta}\,\middle|\,\tilde{\beta} = lT_b^{-1}, l \in Z\right\}$. If $\tilde{\beta}$=0, then $\left|\tilde{\Omega}_r\left(\tilde{\beta},\tilde{\tau}\right)\right|$can be further expressed as

$$\left|\tilde{\Omega}\left(0,\tilde{\tau}\right)\right|=\begin{cases}\left|\Re_i(T_bM)^{-1}e^{j2\pi\Delta f_c\tilde{\tau}}\sum\limits_{p=1}^{M}e^{j2\pi f_\Delta\tilde{s}_p\tau_0}\right.\\ \left.\times\left(U_1\left(0\right)+M^{-1}\sum\limits_{q=1}^{M}U_2((\tilde{s}_q-\tilde{s}_p)\,f_\Delta)\right)\right|,\\ \quad\text{when}\quad|\tilde{\tau}|<T_b\\ \left|\Re_iT_b^{-1}M^{-2}e^{j2\pi\Delta f_c\tilde{\tau}}\sum\limits_{q=1}^{M}\sum\limits_{p=1}^{M}e^{j2\pi f_\Delta\tilde{s}_p\tau_0}\right.\\ \left.\times(U_1((\tilde{s}_q-\tilde{s}_p)f_\Delta)+U_2\left((\tilde{s}_q-\tilde{s}_p)\,f_\Delta\right))\right|,\\ \quad\text{when}\quad|\tilde{\tau}|\geq T_b\end{cases}. \quad (32)$$

According to (32), it is clear that such peaks exist at $\tilde{\tau}=l(2f_\Delta)^{-1}\,(l\in Z)$, and their values are

$$\left|\tilde{\Omega}\left(0,l(2f_\Delta)^{-1}\right)\right|=\begin{cases}\Re_i\left(1-\frac{M-1}{T_bM}\left|l\cdot(2f_\Delta)^{-1}\right|\right),\\ \quad\text{when}\quad\left|l\cdot(2f_\Delta)^{-1}\right|<T_b\\ \Re_iM^{-1},\\ \quad\text{when}\quad\left|l\cdot(2f_\Delta)^{-1}\right|\geq T_b\end{cases}. \quad (33)$$

From (33), it is noted that the magnitude of $\left|\tilde{\Omega}\left(0,l(2f_\Delta)^{-1}\right)\right|$ is dependent upon the modulation order M, the frequency deviation f_Δ and the symbol period T_b. Furthermore, for any given M, the maximum peak value of the magnitudes of the $\left|\tilde{\Omega}\left(0,l(2f_\Delta)^{-1}\right)\right|$ can be reached for $l\cdot(2f_\Delta)^{-1}=0$. It can be further noticed from (33) that the magnitude of $\left|\tilde{\Omega}\left(0,l(2f_\Delta)^{-1}\right)\right|$ decreases with an increase in time delay $\tilde{\tau}$ for $\left|l\cdot(2f_\Delta)^{-1}\right|<T_b$ and the magnitude of $\left|\tilde{\Omega}\left(0,l(2f_\Delta)^{-1}\right)\right|$ remains constant if and only if $\left|l\cdot(2f_\Delta)^{-1}\right|\geq T_b$. This distinctive feature of the magnitude of $\left|\tilde{\Omega}\left(0,l(2f_\Delta)^{-1}\right)\right|$ is exploited to develop an algorithm for estimating T_b. From the above, it can be shown that the magnitude of the generalized second-order cyclic moment for M-FSK signals is dependent on the symbol period T_b, and the problem of blind symbol period estimation can be solved by generalized cyclostationarity-based algorithm.

APPENDIX D
PROOF OF PROPOSITION 3

The expected value of $\hat{\vartheta}_s(\varepsilon)$ is given by

$$E\left\{\hat{\vartheta}_s\left(\varepsilon\right)\right\}=\frac{1}{KC_\vartheta}\sum_{k=0}^{K-1}E\left\{s\left(k\right)\right\}e^{-j2\pi k\varepsilon/K}, \quad (34)$$

where $C_\vartheta=\left(|\rho_hA|+\Delta^2\right)$. From (34), it can be seen that the magnitude of $E\left\{\hat{\vartheta}_s\left(\varepsilon\right)\right\}$ is dependent on C_ϑ. If $K\to\infty$, we obtain

$$\lim_{K\to\infty}E\left\{\hat{\vartheta}_s\left(\varepsilon\right)\right\}=\xi_s\left(\varepsilon\right), \quad (35)$$

where $\xi_s(\varepsilon)=\frac{1}{K}\sum_{k=0}^{K-1}s(k)e^{-j2\pi k\varepsilon/K}$. Based on (35), $\hat{\vartheta}_s(\varepsilon)$ is an asymptotic unbiased estimate of $\xi_s\left(\varepsilon\right)$.

The expected value of $\hat{\vartheta}_r^2\left(\varepsilon\right)$ is given as

$$\begin{aligned}E\left\{\hat{\vartheta}_s^2(\varepsilon)\right\}&=E\left\{\left(\frac{1}{KC_\vartheta}\sum_{k=0}^{K-1}s\left(k\right)e^{-j2\pi k\varepsilon/K}\right)^2\right\}\\&=\frac{1}{C_\vartheta^2}E\left\{\left(\frac{1}{K}\sum_{k=0}^{K-1}s\left(k\right)e^{-j2\pi k\varepsilon/K}\right)^2\right\}\\&=\frac{1}{C_\vartheta^2}E\left\{\xi_s^2\left(\varepsilon\right)\right\}.\end{aligned} \quad (36)$$

Employing (34) and (36), one obtain

$$\lim_{K\to\infty}\mathrm{var}\left[\hat{\vartheta}_s^2\left(\varepsilon\right)\right]=\lim_{K\to\infty}\left(E\left\{\hat{\vartheta}_s^2\left(\varepsilon\right)\right\}-E^2\left\{\hat{\vartheta}_s\left(\varepsilon\right)\right\}\right)=0. \quad (37)$$

According to Chebyshev inequality, it can be seen that the estimator of generalized first-order cyclic moment is consistent.

APPENDIX E
PROOF OF PROPOSITION 4

The expected value of $\hat{\Omega}_s\left(\beta,\upsilon\right)$ can be expressed as

$$E\left\{\hat{\Omega}_s(\beta,\tau)\right\}=\frac{\Upsilon_\Omega}{K}\sum_{k=0}^{K-1}E\{s(k)s(k+\tau)\}e^{-j2\pi k\beta/K}, \quad (38)$$

where $\Upsilon_\Omega=\left(|\rho_hA|+\Delta^2\right)^{-2}$. The result from (38) illustrates that the magnitude of $E\left\{\hat{\Omega}_s\left(\beta,\tau\right)\right\}$ is dependent on Υ_Ω. If $K\to\infty$, we obtain

$$\lim_{K\to\infty}E\left\{\hat{\Omega}_s\left(\beta,\tau\right)\right\}=\zeta_s\left(\beta,\tau\right). \quad (39)$$

where $\zeta_s\left(\beta,\tau\right)=\frac{1}{K}\sum_{k=0}^{K-1}s\left(k\right)s\left(k+\tau\right)e^{-j2\pi k\beta/K}$. Based on (39), $\hat{\Omega}_s\left(\beta,\tau\right)$ is an asymptotic unbiased estimate of $\zeta_s\left(\beta,\tau\right)$.

The expected value of $\hat{\Omega}_s^2\left(\beta,\tau\right)$ can be written as

$$\begin{aligned}E\left\{\hat{\Omega}_s^2\left(\beta,\tau\right)\right\}&=E\left\{\left(\frac{\Upsilon_\Omega}{K}\sum_{k=0}^{K-1}x(k)x^*(k+\tau)e^{-j2\pi k\beta/K}\right)^2\right\}\\&=\Upsilon_\Omega E\left\{\zeta_s^2\left(\beta,\tau\right)\right\}.\end{aligned} \quad (40)$$

Based on (38) and (40), one obtain

$$\begin{aligned}&\lim_{K\to\infty}\mathrm{var}\left[\hat{\Omega}_s^2\left(\beta,\tau\right)\right]\\&=\lim_{K\to\infty}E\left\{\hat{\Omega}_s^2\left(\beta,\tau\right)\right\}-\lim_{K\to\infty}E^2\left\{\hat{\Omega}_s^2\left(\beta,\tau\right)\right\}=0.\end{aligned} \quad (41)$$

According to Chebyshev inequality, it can be seen that the estimator of generalized second-order cyclic moment is consistent.

APPENDIX F
PROOF OF LEMMA 2

According to the basic idea of the generalized cyclostationarity, we first construct the nonlinear transformation,

$$f\left[r(t)\right]=\frac{r(t)}{|r(t)|+\Delta^2}, \quad (42)$$

where $r(t)$ is received signal, and Δ represents compression factor. Then, the first-order time-varying moment of $f[r(t)]$ is defined as

$$\begin{aligned} C_r(t) &= E\{f[r(t)]\} \\ &= E\left\{\frac{r(t)}{|r(t)|+\Delta^2}\right\} \\ &= E\left\{\frac{\tilde{s}(t)+w(t)}{|\tilde{s}(t)+w(t)|+\Delta^2}\right\} \\ &= E\left[\frac{\tilde{s}(t)}{|\tilde{s}(t)+w(t)|+\Delta^2}+\frac{w(t)}{|\tilde{s}(t)+w(t)|+\Delta^2}\right], \end{aligned} \tag{43}$$

where $\tilde{s}(t) = h(t) \otimes s(t)$, $E\{\cdot\}$, $E\{\cdot\}$ is the mean operator.

When MSNR is high, equation (43) can be approximately expressed as

$$\begin{aligned} C_r(t) &= E\{f[r(t)]\} \\ &\approx E\left\{\frac{\tilde{s}(t)}{|\tilde{s}(t)|+\Delta^2}+\frac{w(t)}{|\tilde{s}(t)|+\Delta^2}\right\} \\ &= C_s^h(t)+C_w^h(t). \end{aligned} \tag{44}$$

where $C_s^h(t) = E\left\{\frac{\tilde{s}(t)}{|\tilde{s}(t)|+\Delta^2}\right\}$ and $C_w^h(t) = E\left\{\frac{w(t)}{|\tilde{s}(t)|+\Delta^2}\right\}$. According to Lemma 1, $C_w^h(t) = E\left\{\frac{w(t)}{|\tilde{s}(t)|+\Delta^2}\right\}$ is finite value, and it is approximately considered as a Gaussian process when $|\tilde{s}(t)| \gg |w(t)|$. Hence, $C_s(t)$ is important role in (44), and $C_r(t)$ can be written as

$$C_r(t) \approx C_s^h(t) = E\left\{\frac{\tilde{s}(t)}{|\tilde{s}(t)|+\Delta^2}\right\}. \tag{45}$$

We consider flat fading channel, that is $\tilde{s}(t) = \rho_h s(t)$, where ρ_h is the channel gain. In this case, $C_r(t)$ can be expressed as

$$\begin{aligned} C_r(t) &\approx E\left\{\frac{\tilde{s}(t)}{|\tilde{s}(t)|+\Delta^2}\right\} \\ &= \Lambda_h \sum_{m=1}^{M}\left(e^{j2\pi f_\Delta \tilde{s}_m t} g(t) \otimes \sum_i \delta(t-iT_b)\right) e^{j2\pi\Delta f_c t}, \end{aligned} \tag{46}$$

where $\Lambda_h = \frac{\rho_h A e^{j\theta} M^{-1}}{|A|+\Delta^2}$, $\otimes$ represents the convolution operator, and $\delta(\cdot)$ is the Dirac delta function. The Fourier transform of $C_r(t)$ can be expressed as in (47).

Based on the result of analysis in [11], $\Im\{C_r(t)\} \neq 0$ when $\tilde{\varepsilon} = \Delta f_c + iT_b^{-1}$, and it can be easily expressed as

$$\begin{aligned} \Im\{C_r(t)\} \approx \Lambda_h T_b^{-1} \sum_{m=1}^{M}\sum_i \delta\left(\tilde{\varepsilon}-\Delta f - iT_b^{-1}\right) \\ \times \int_{-\infty}^{\infty} g(\iota)\, e^{j2\pi f_\Delta \tilde{s}_m \iota} e^{-j2\pi i \iota T_b^{-1}} d\iota. \end{aligned} \tag{48}$$

If the product $f_\Delta \tilde{s}_m$ is an integer of T_b^{-1}, that is, $f_\Delta \tilde{s}_m = \rho T_b^{-1}$, with ρ as an integer. $\Im\{C_r(t)\}$ can be rewritten as follows

$$\Im\{C_r(t)\} \approx \Lambda_h \sum_{\rho\in \mathrm{P}} \delta\left(\tilde{\varepsilon}-\Delta f_c - \rho T_b^{-1}\right), \tag{49}$$

where $\{\rho = f_\Delta \tilde{s}_m T_b, \rho \in Z, \tilde{s}_m = 2m-1-M\}$. If the M-SNR is low, equation (43) can be approximately written as

$$\begin{aligned} C_r(t) &= E\{f[r(t)]\} \\ &\approx E\left\{\frac{\tilde{s}(t)}{|w(t)|+\Delta^2}+\frac{w(t)}{|w(t)|+\Delta^2}\right\} \\ &= C_s^l(t)+C_w^l(t). \end{aligned} \tag{50}$$

where $C_s^l(t) = E\left\{\frac{\tilde{s}(t)}{|w(t)|+\Delta^2}\right\}$ and $C_w^l(t) = E\left\{\frac{w(t)}{|w(t)|+\Delta^2}\right\}$. In (50), $C_s^l(t)$ contains the information of mixture signal-to-noise, in other words, the amplitude of $C_s^l(t)$ decreases with decreasing the MSNR. $C_w^l(t)$ represents the mean of $f[w(t)]$, and it is finite value. When $|w(t)| \gg |\tilde{s}(t)|$, $\frac{w(t)}{|w(t)|+\Delta^2}$ is the approximate amplitude normalization, and it can be approximated as a Gaussian process, that is $C_w^l(t) \approx 0$. We can rewrite $C_r(t)$ as

$$C_r(t) \approx C_s^l(t) = E\left\{\frac{\tilde{s}(t)}{|w(t)|+\Delta^2}\right\}. \tag{51}$$

For low MSNR, the derivation and analysis process is similar to that under high MSNR. When $f_\Delta \tilde{s}_m = \rho T_b^{-1}$, with ρ as an integer, the generalized first order cyclic moment $\Im\{C_r(t)\}$ can be expressed as follows

$$\Im\{C_r(t)\} \approx \Lambda_l \sum_{\rho\in \mathrm{P}} \delta\left(\tilde{\varepsilon}-\Delta f_c - \rho T_b^{-1}\right), \tag{52}$$

where $\Lambda_l = \frac{\rho_h A e^{j\theta} M^{-1}}{|w(t)|+\Delta^2}$ and $\{\rho = f_\Delta \tilde{s}_m T_b, \rho \in Z, \tilde{s}_m = 2m-1-M\}$.

APPENDIX G
PROOF OF LEMMA 3

According to the generalized cyclostationarity, the generalized the second-order time-varying moment of $f[r(t)]$ can be expressed as in (53).

$$\begin{aligned} G_r(t,\tilde{\tau}) &= E\{f[r(t)]\, f^*[r(t-\tilde{\tau})]\} \\ &= E\left\{\left(\frac{r(t)}{|r(t)|+\Delta^2}\right)\left(\frac{r(t-\tilde{\tau})}{|r(t-\tilde{\tau})|+\Delta^2}\right)^*\right\} \\ &= E\left\{\left(\frac{\tilde{s}(t)+w(t)}{|\tilde{s}(t)+w(t)|+\Delta^2}\right) \right. \\ &\left. \times\left(\frac{\tilde{s}(t-\tilde{\tau})+w(t-\tilde{\tau})}{|\tilde{s}(t-\tilde{\tau})+w(t-\tilde{\tau})|+\Delta^2}\right)^*\right\} \\ &= E\left\{\frac{\tilde{s}(t)\tilde{s}^*(t-\tilde{\tau})}{(|\tilde{s}(t)+w(t)|+\Delta^2)(|\tilde{s}(t-\tilde{\tau})+w(t-\tilde{\tau})|+\Delta^2)}\right. \\ &\left. + \frac{w(t)w^*(t-\tilde{\tau})}{(|\tilde{s}(t)+w(t)|+\Delta^2)(|\tilde{s}(t-\tilde{\tau})+w(t-\tilde{\tau})|+\Delta^2)}\right\} \end{aligned} \tag{53}$$

In (53), $\tilde{\tau}$ denotes the time delay delay, and $*$ represents the complex conjugate.

Let us assume that MSNR is high, we can approximate

$$\begin{aligned}\Im\left\{C_r(t)\right\} &\approx \int_{-\infty}^{\infty}\Lambda_h\sum_{m=1}^{M}\left(e^{j2\pi f_\Delta \tilde{s}_m t}g(t)\otimes\sum_i\delta(t-iT_b)\right)\times e^{j2\pi\Delta f_c t}e^{-j2\pi\tilde{\varepsilon}t}dt \\ &= \Lambda_h\int_{-\infty}^{\infty}\sum_{m=1}^{M}e^{j2\pi f_\Delta \tilde{s}_m \iota}g\left(\iota\right)\times\int_{-\infty}^{\infty}\sum_i\delta\left(t-\iota-iT_b\right)e^{-j2\pi(\tilde{\varepsilon}-\Delta f_c)t}dtd\iota,\end{aligned} \tag{47}$$

$G_r\left(t,\tilde{\tau}\right)$ as

$$\begin{aligned}&G_r\left(t,\tilde{\tau}\right)=E\left\{f\left[r(t)\right]f^*\left[r\left(t-\tilde{\tau}\right)\right]\right\}\\&\approx E\left\{\frac{\tilde{s}(t)\tilde{s}^*\left(t-\tilde{\tau}\right)}{|\tilde{s}(t)|\,|\tilde{s}\left(t-\tilde{\tau}\right)|+\Delta^2}+\frac{w(t)w^*\left(t-\tilde{\tau}\right)}{|\tilde{s}(t)|\,|\tilde{s}\left(t-\tilde{\tau}\right)|+\Delta^2}\right\}\\&=E\left\{\frac{\tilde{s}(t)\tilde{s}^*\left(t-\tilde{\tau}\right)}{\left|\tilde{s}(t)\right|^2+\Delta^2}\right\}\\&+E\left\{\frac{w(t)w^*\left(t-\tilde{\tau}\right)}{\left|\tilde{s}(t)\right|^2+\Delta^2}\right\}.\end{aligned} \tag{54}$$

Equation (54) can be further expressed as

$$\begin{aligned}G_r\left(t,\tilde{\tau}\right)&=E\left\{f\left[r(t)\right]f^*\left[r\left(t-\tilde{\tau}\right)\right]\right\}\\&\approx G_s^h\left(t,\tilde{\tau}\right)+G_w^h\left(t,\tilde{\tau}\right),\end{aligned} \tag{55}$$

where $G_s^h\left(t,\tilde{\tau}\right)=E\left\{\frac{\tilde{s}(t)\tilde{s}^*(t-\tilde{\tau})}{|\tilde{s}(t)|^2+\Delta^2}\right\}$ retains the frequency characteristics of the transmitter signal, and $G_w^h\left(t,\tilde{\tau}\right)=E\left\{\frac{w(t)w^*(t-\tilde{\tau})}{|\tilde{s}(t)|^2+\Delta^2}\right\}$ contains the information of mixture signal-to-noise ratio. For $|\tilde{s}(t)|\gg|w(t)|$, the second order moments of $\frac{w(t)w^*(t-\tilde{\tau})}{|\tilde{s}(t)|^2+\Delta^2}$ are finite, and it can be approximated as a Gaussian process. Hence, $C_w^h(t)$ can be ignored in (55), that is, $G_r\left(t,\tilde{\tau}\right)$ can be simplified to

$$G_r\left(t,\tilde{\tau}\right)\approx E\left\{\frac{\tilde{s}(t)\tilde{s}^*\left(t-\tilde{\tau}\right)}{\left|\tilde{s}(t)\right|^2+\Delta^2}\right\}, \tag{56}$$

We consider flat fading channel, that is $\tilde{s}(t)=\rho_h s(t)$, where ρ_h is the channel gain. The generalized second-order cyclic moment for M-FSK signal can be written as in (57).

According to the derivation process in [14], $G_r\left(t,\tilde{\tau}\right)$ can be expressed as in (58). In equation (58), $\Re_h=\frac{(\rho_h A)^2}{|\rho_h A|^2+\Delta^2}$ and $\tilde{s}_p\in\{2p-1-M,p=1,\cdots,M\}$, $\tilde{s}_q\in\{2q-1-M,q=1,\cdots,M\}$, $\tilde{s}_p$ and $\tilde{s}_q$ are independently and identically distributed random variables.

The generalized second-order cyclic moment can be obtained as the Fourier transform of the $G_r\left(t,\tilde{\tau}\right)$, as in (59). In equation (59), $U_1\left(\tilde{\beta}\right)$, $U_2\left(\tilde{\beta}\right)$ are the Fourier transforms of $g(t)g\left(t-\tau_0\right)$ and $g(t)g\left(t+\mu T_b-\tau_0\right)$, given respectively by in (60).

$$\begin{aligned}U_1\left(\tilde{\beta}\right)&=\left(T_b-|\tau_0|\right)\left[\mathrm{sinc}\left(\left(T_b-|\tau_0|\right)\tilde{\beta}\right)\right]e^{-j\pi\tilde{\beta}(T_b+\mu|\tau_0|)},\\U_2\left(\tilde{\beta}\right)&=|\tau_0|\left[\mathrm{sinc}\left(|\tau_0|\tilde{\beta}\right)\right]e^{-j\pi\tilde{\beta}(T_b+\mu(|\tau_0|-T_b))}.\end{aligned} \tag{60}$$

When the MSNR is low, we can express equation (55) approximately as

$$\begin{aligned}&G_r\left(t,\tilde{\tau}\right)=E\left\{f\left[r(t)\right]f^*\left[r\left(t-\tilde{\tau}\right)\right]\right\}\\&\approx E\left\{\frac{\tilde{s}(t)\tilde{s}^*\left(t-\tilde{\tau}\right)}{|w(t)|\,|w\left(t-\tilde{\tau}\right)|+\Delta^2}+\frac{w(t)w^*\left(t-\tilde{\tau}\right)}{|w(t)|\,|w\left(t-\tilde{\tau}\right)|+\Delta^2}\right\}\\&=E\left\{\frac{\tilde{s}(t)\tilde{s}^*\left(t-\tilde{\tau}\right)}{|w(t)|^2+\Delta^2}\right\}+E\left\{\frac{w(t)w^*\left(t-\tilde{\tau}\right)}{|w(t)|^2+\Delta^2}\right\}.\end{aligned} \tag{61}$$

$G_r\left(t,\tilde{\tau}\right)$ is further given as

$$\begin{aligned}G_r\left(t,\tilde{\tau}\right)&=E\left\{f\left[r(t)\right]f^*\left[r\left(t-\tilde{\tau}\right)\right]\right\}\\&\approx G_s^l\left(t,\tilde{\tau}\right)+G_w^l\left(t,\tilde{\tau}\right),\end{aligned} \tag{62}$$

where $G_s^l\left(t,\tilde{\tau}\right)=E\left\{\frac{\tilde{s}(t)\tilde{s}^*(t-\tilde{\tau})}{|w(t)|^2+\Delta^2}\right\}$ and $G_w^l\left(t,\tilde{\tau}\right)=E\left\{\frac{w(t)w^*(t-\tilde{\tau})}{|w(t)|^2+\Delta^2}\right\}$. When $|w(t)|\gg|\tilde{s}(t)|$, the amplitude of $G_s^l\left(t,\tilde{\tau}\right)$ is dependent on the amplitude of $|\tilde{s}(t)|$ and $|w(t)|$, and it decreases with decreasing the MSNR. In addition, we note that the amplitude of $w(t)$ is approximately normalized by the nonlinear transformation in $G_s^l\left(t,\tilde{\tau}\right)$, and $\frac{w(t)w^*(t-\tilde{\tau})}{|w(t)|^2+\Delta^2}$ can be approximated as a Gaussian process. Hence, $C_w^l(t)\approx 0$, and $G_r\left(t,\tilde{\tau}\right)$ can be rewritten as

$$G_r\left(t,\tilde{\tau}\right)\approx G_s^l\left(t,\tilde{\tau}\right), \tag{63}$$

When the MSNR is low, the generalized second-order cyclic moment $\tilde{\Omega}_r\left(\tilde{\beta},\tilde{\tau}\right)$ is given as in(64)). In equation (64), $\Re_l=\frac{(\rho_h A)^2}{|w(t)|^2+\Delta^2}$.

REFERENCES

[1] M. Liu, L. Liu, H. Song, Y. Hu, Y. Yi, and F. Gong, "Signal estimation in underlay cognitive networks for industrial internet of things," *IEEE Transactions on Industrial Informatics*, vol. 16, no. 8, pp. 5478–5488, 2020.

[2] M. Liu, G. Liao, Z. Yang, H. Song, and F. Gong, "Electromagnetic signal classification based on deep sparse capsule networks," *IEEE Access*, vol. 7, pp. 83 974–83 983, 2019.

[3] M. Liu, J. Zhang, Y. Lin, Z. Wu, B. Shang, and F. Gong, "Carrier frequency estimation of time-frequency overlapped MASK signals for underlay cognitive radio network," *IEEE Access*, vol. 7, pp. 58 277–58 285, 2019.

[4] K. Ho, W. Prokopiw, and Y. Chan, "Modulation identification of digital signals by the wavelet transform," *IEE Proceedings-Radar, Sonar and Navigation*, vol. 147, no. 4, pp. 169–176, 2000.

[5] X. Jun, W. Fu-ping, and W. Zan-ji, "The improvement of symbol rate estimation by the wavelet transform," in *Proceedings. 2005 International Conference on Communications, Circuits and Systems, 2005.*, vol. 1. IEEE, 2005, pp. 100–103.

[6] Y. Gao, Y. Wan, L. Li, and J. Men, "Baud rate estimation of FSK signals based on wavelet transform," in *2012 Second International Conference on Intelligent System Design and Engineering Application*. IEEE, 2012, pp. 181–184.

[7] L. Hong and K. Ho, "Identification of digital modulation types using the wavelet transform," in *MILCOM 1999. IEEE Military Communications. Conference Proceedings (Cat. No. 99CH36341)*, vol. 1. IEEE, 1999, pp. 427–431.

$$
\begin{aligned}
G_r\left(t,\tilde{\tau}\right) &\approx E\left\{\frac{\tilde{s}(t)\tilde{s}^*\left(t-\tilde{\tau}\right)}{\left|\tilde{s}(t)\right|^2+\Delta^2}\right\} \\
&= E\left\{\frac{\left(\rho_h A\right)^2 \sum\limits_i e^{j2\pi f_\Delta s_i(t-iT_b)} g(t-iT_b) e^{j2\pi\Delta f_c t} \sum\limits_n e^{-j2\pi f_\Delta s_n(t-nT_b-\tilde{\tau})} g(t-nT_b-\tilde{\tau}) e^{-j2\pi\Delta f_c(t-\tilde{\tau})}}{\left|\rho_h A\right|^2+\Delta^2}\right\} \\
&= \frac{\left(\rho_h A\right)^2}{\left|\rho_h A\right|^2+\Delta^2} E\left\{e^{j2\pi\Delta f_c\tilde{\tau}} \sum_i e^{j2\pi f_\Delta s_i(t-iT_b)} g\left(t-iT_b\right) \sum_n e^{-j2\pi f_\Delta s_n(t-nT_b-\tilde{\tau})} g(t-nT_b-\tilde{\tau})\right\}.
\end{aligned} \tag{57}
$$

$$
G_s(t,\tilde{\tau}) = \begin{cases}
\Re_h M^{-1} e^{j2\pi\Delta f_c\tilde{\tau}} \sum\limits_i \sum\limits_{p=1}^{M} e^{j2\pi f_\Delta \tilde{s}_p\tau_0} \left[g\left(t-iT_b\right) g\left(t-iT_b-\tau_0\right)\right. \\
\left. M^{-1} \sum\limits_{q=1}^{M} e^{j2\pi f_\Delta(\tilde{s}_q-\tilde{s}_p)(t-iT)} g\left(t-iT_b\right) g\left(t-(i-\mu)T_b-\tau_0\right)\right], \quad \text{when} \quad |\tilde{\tau}| < T_b \\
\Re_h M^{-2} e^{j2\pi\Delta f_c\tilde{\tau}} \sum\limits_i \sum\limits_{q=1}^{M} \sum\limits_{p=1}^{M} e^{j2\pi f_\Delta(\tilde{s}_q-\tilde{s}_p)(t-iT_b)} e^{j2\pi f_\Delta \tilde{s}_p\tau_0} \\
\times\left[g\left(t-iT_b\right) g\left(t-iT_b-\tau_0\right) + g\left(t-iT_b\right) g\left(t-(i-\mu)T_b-\tau_0\right)\right], \quad \text{when} \quad |\tilde{\tau}| \geq T_b
\end{cases}. \tag{58}
$$

$$
\tilde{\Omega}_r\left(\tilde{\beta},\tilde{\tau}\right) = \Im\{G_r\left(t,\tilde{\tau}\right)\} \approx \begin{cases}
\Re_h (T_b M)^{-1} e^{j2\pi\Delta f_c\tilde{\tau}} \sum\limits_{p=1}^{M} e^{j2\pi f_\Delta \tilde{s}_p\tau_0} \\
\times\left(U_1\left(\tilde{\beta}\right) + M^{-1} \sum\limits_{q=1}^{M} U_2\left(\tilde{\beta}-(\tilde{s}_q-\tilde{s}_p)f_\Delta\right)\right), \quad \text{when} \quad |\tilde{\tau}| < T_b \\
\Re_h T_b^{-1} M^{-2} e^{j2\pi\Delta f_c\tilde{\tau}} \sum\limits_{q=1}^{M} \sum\limits_{p=1}^{M} e^{j2\pi f_\Delta \tilde{s}_p\tau_0} e^{j2\pi f_\Delta \tilde{s}_p\tau_0} \\
\times\left(U_1\left(\tilde{\beta}-(\tilde{s}_q-\tilde{s}_p)f_\Delta\right) + U_2\left(\tilde{\beta}-(\tilde{s}_q-\tilde{s}_p)f_\Delta\right)\right), \quad \text{when} \quad |\tilde{\tau}| \geq T_b
\end{cases}. \tag{59}
$$

$$
\tilde{\Omega}_r\left(\tilde{\beta},\tilde{\tau}\right) = \Im\{G_r\left(t,\tilde{\tau}\right)\} \approx \begin{cases}
\Re_l (T_b M)^{-1} e^{j2\pi\Delta f_c\tilde{\tau}} \sum\limits_{p=1}^{M} e^{j2\pi f_\Delta \tilde{s}_p\tau_0} \\
\times\left(U_1\left(\tilde{\beta}\right) + M^{-1} \sum\limits_{q=1}^{M} U_2\left(\tilde{\beta}-(\tilde{s}_q-\tilde{s}_p)f_\Delta\right)\right), \quad \text{when} \quad |\tilde{\tau}| < T_b \\
\Re_l T_b^{-1} M^{-2} e^{j2\pi\Delta f_c\tilde{\tau}} \sum\limits_{q=1}^{M} \sum\limits_{p=1}^{M} e^{j2\pi f_\Delta \tilde{s}_p\tau_0} e^{j2\pi f_\Delta \tilde{s}_p\tau_0} \\
\times\left(U_1\left(\tilde{\beta}-(\tilde{s}_q-\tilde{s}_p)f_\Delta\right) + U_2\left(\tilde{\beta}-(\tilde{s}_q-\tilde{s}_p)f_\Delta\right)\right), \quad \text{when} \quad |\tilde{\tau}| \geq T_b
\end{cases}. \tag{64}
$$

[8] J. Chen, Y. Kuo, J. Li, F. Fu, and Y. Ma, "Digital modulation identification by wavelet analysis," in *Sixth International Conference on Computational Intelligence and Multimedia Applications (ICCIMA'05)*. IEEE, 2005, pp. 29–34.

[9] Z. Yu, Y. Q. Shi, and W. Su, "M-ary frequency shift keying signal classification based-on discrete fourier transform," in *IEEE Military Communications Conference, 2003. MILCOM 2003.*, vol. 2. IEEE, 2003, pp. 1167–1172.

[10] A. E. El-Mahdy and N. M. Namazi, "Classification of multiple m-ary frequency-shift keying signals over a rayleigh fading channel," *IEEE Transactions on Communications*, vol. 50, no. 6, pp. 967–974, 2002.

[11] O. A. Dobre, S. Rajan, and R. Inkol, "Joint signal detection and classification based on first-order cyclostationarity for cognitive radios," *EURASIP Journal on Advances in Signal Processing*, vol. 2009, pp. 1–12, 2009.

[12] O. A. Dobre, S. Rajan, and R. Inkol, "A novel algorithm for blind recognition of M-ary frequency shift keying modulation," in *2007 IEEE Wireless Communications and Networking Conference*. IEEE, 2007, pp. 520–524.

[13] H. Wang, O. A. Dobre, C. Li, and R. Inkol, "M-FSK signal recognition in fading channels for cognitive radio," in *2012 IEEE Radio and Wireless Symposium*. IEEE, 2012, pp. 375–378.

[14] H. Wang, O. A. Dobre, C. Li, and D. C. Popescu, "Blind cyclostationarity-based symbol period estimation for FSK signals," *IEEE Communications Letters*, vol. 19, no. 7, pp. 1149–1152, 2015.

[15] Y. M. Chee, A. Z. Shaąfameri, and M. M. A. Zabidi, "If estimation of FSK signals using adaptive smoothed windowed cross wigner–ville distribution," *Signal processing*, vol. 100, pp. 71–84, 2014.

[16] Á. Navia-Vazquez and J. Arenas-Garcia, "Combination of recursive least p-norm algorithms for robust adaptive filtering in alpha-stable noise," *IEEE Transactions on Signal Processing*, vol. 60, no. 3, pp. 1478–1482, 2011.

[17] Y. Chen and J. Chen, "Novel SαS PDF approximations and their applications in wireless signal detection," *IEEE Transactions on Wireless Communications*, vol. 14, no. 2, pp. 1080–1091, 2014.

[18] A. Mahmood, M. Chitre, and M. A. Armand, "On single-carrier communication in additive white symmetric alpha-stable noise," *IEEE Transactions on Communications*, vol. 62, no. 10, pp. 3584–3599, 2014.

[19] A. Mahmood, M. Chitre, and M. A. Armand, "Detecting OFDM signals in alpha-stable noise," *IEEE Transactions on Communications*, vol. 62, no. 10, pp. 3571–3583, 2014.
[20] J. Friedmann, H. Messer, and J.-F. Cardoso, "Robust parameter estimation of a deterministic signal in impulsive noise," *IEEE transactions on Signal Processing*, vol. 48, no. 4, pp. 935–942, 2000.
[21] K. Pelekanakis and M. Chitre, "Adaptive sparse channel estimation under symmetric alpha-stable noise," *IEEE Transactions on wireless communications*, vol. 13, no. 6, pp. 3183–3195, 2014.
[22] R. Hu, Y. Fu, Z. Chen, Y. Xiang, and R. Rong, "Robust sparse signal recovery in the presence of the α noise," *IEEE Signal Processing Letters*, vol. 23, no. 11, pp. 1687–1691, 2016.
[23] J. He, P. Du, and X. Chen, "Parameter estimation of communication signal in alpha-stable distribution noise environment," in *2017 13th International Conference on Computational Intelligence and Security (CIS)*. IEEE, 2017, pp. 182–186.
[24] G. Yang, J. Wang, G. Zhang, Q. Shao, and S. Li, "Joint estimation of timing and carrier phase offsets for MSK signals in alpha-stable noise," *IEEE Communications Letters*, vol. 22, no. 1, pp. 89–92, 2017.
[25] C. Qian, Y. Shi, L. Huang, and H. C. So, "Robust harmonic retrieval via block successive upper-bound minimization," *IEEE Transactions on Signal Processing*, vol. 66, no. 23, pp. 6310–6324, 2018.
[26] G. Yang, J. Wang, G. Zhang, and S. Li, "Communication signal pre-processing in impulsive noise: A bandpass myriad filtering-based method," *IEEE Communications Letters*, vol. 22, no. 7, pp. 1402–1405, 2018.
[27] Y. Hou, R. Liu, B. Dai, and L. Zhao, "Joint channel estimation and LDPC decoding over time-varying impulsive noise channels," *IEEE Transactions on Communications*, vol. 66, no. 6, pp. 2376–2383, 2018.
[28] L. Lu, H. Zhao, and B. Champagne, "Distributed nonlinear system identification in α-stable noise," *IEEE Signal Processing Letters*, vol. 25, no. 7, pp. 979–983, 2018.
[29] S. P. Talebi, S. Werner, and D. P. Mandic, "Distributed adaptive filtering of α-stable signals," *IEEE Signal Processing Letters*, vol. 25, no. 10, pp. 1450–1454, 2018.
[30] M. Liu, N. Zhao, J. Li, and V. C. M. Leung, "Spectrum sensing based on maximum generalized correntropy under symmetric alpha stable noise," *IEEE Transactions on Vehicular Technology*, vol. 68, no. 10, pp. 10 262–10 266, 2019.
[31] M. Liu, J. Zhang, and B. Li, "Symbol rates estimation of time-frequency overlapped MPSK signals for underlay cognitive radio network," *IEEE Access*, vol. 6, pp. 16 216–16 223, 2018.